Blocking and Routing Discrete Solitons in Two-Dimensional Networks of Nonlinear Waveguide Arrays

Demetrios N. Christodoulides and Eugenia D. Eugenieva
Department of Electrical and Computer Engineering, Lehigh University, Bethlehem, Pennsylvania 18015
(Received 25 April 2001; published 15 November 2001)

It is shown that discrete solitons can be navigated in two-dimensional networks of nonlinear waveguide arrays. This can be accomplished via vector interactions between two classes of discrete solitons: signals and blockers. Discrete solitons in such two-dimensional networks can exhibit a rich variety of functional operations, e.g., blocking, routing, logic functions, and time gating.

DOI: 10.1103/PhysRevLett.87.233901 PACS numbers: 42.65.Tg, 42.79.Ta

Discrete solitons in nonlinear lattices have been the focus of considerable attention in diverse branches of science [1–5]. These solitons are possible in several physical settings such as, for example, biological systems [1], nonlinear optics [2], solid state physics [3], and Bose-Einstein condensates [4]. In optics, discrete solitons were first predicted in nonlinear waveguide arrays in 1988 [2] and were successfully observed a decade later [5]. In this system, discrete localized states are possible by balancing the effect of discrete diffraction (arising from the coupling between neigboring waveguides) with that of material nonlinearity. As pointed out in a number of studies, optical discrete solitons differ fundamentally from their bulk counterparts in several ways [6–9]. For example, a unique property that follows from the discrete nature of waveguide arrays is that of reverse diffraction; this leads to the exciting possibility of observing dark solitons in self-focusing Kerr media [10].

The prospect of using discrete solitons (DSs) in single-row (linear) waveguide arrays for data processing applications has been raised. However, by their very nature (i.e., because of their one-dimensional topology), the functionality of linear waveguide networks for signal manipulation purposes is considerably limited. Thus, it would be highly desirable to introduce new geometrical arrangements capable of exhibiting superior performance in terms of realizing intelligent operations.

In this Letter we show that discrete optical solitons propagating in two-dimensional waveguide array networks can provide a rich environment for all-optical data processing applications. We demonstrate that such arrays effectively act like *soliton wires* along which these self-trapped entities can travel. In addition, by using vector/incoherent interactions at network junctions, soliton signals can be routed at will on specific pathways. Therefore, this family of solitons can be *navigated* anywhere within a two-dimensional network of nonlinear waveguides. The possibility of realizing useful functional operations such as blocking, routing, logic functions, and time gating is discussed.

We begin our analysis by considering a two-dimensional network of nonlinear waveguide arrays involving identical elements. Each branch is composed of regularly spaced waveguides, separated by each other by distance D, as shown in Fig. 1(a). The index profile of a single waveguide along with its linear mode is depicted in Figs. 1(b) and 1(c). Every waveguide is designed to be single moded at the operating wavelength [11]. To make the discussion more relevant, let us assume that the cladding refractive index is $n_0 = 1.5$, and that the wavelength used is $\lambda_0 = 1.5\ \mu$m. The linear refractive index difference between the core and cladding is taken to be $\delta = 3 \times 10^{-3}$, and the effective core radius is 5.3 μm. The distance between waveguides is 15.9 μm, which results in a linear coupling constant $c = 0.279\ \text{mm}^{-1}$ between nearest neighbors. Note that the actual set of values used here is not crucial to this discussion since the problem itself can always be scaled. In addition, we assume that the material is Kerr nonlinear and that it supports vector or incoherent interactions between two fields [12–14]. In this case, the two field envelopes (propagating along z) evolve according to

$$i\frac{\partial U}{\partial z} + \frac{1}{2k}\left(\frac{\partial^2 U}{\partial x^2} + \frac{\partial^2 U}{\partial y^2}\right) + \frac{k\delta f(x,y)}{n_0}U + \frac{kn_2I_0}{n_0}(|U|^2 + \alpha|V|^2)U = 0, \tag{1a}$$

$$i\frac{\partial V}{\partial z} + \frac{1}{2k}\left(\frac{\partial^2 V}{\partial x^2} + \frac{\partial^2 V}{\partial y^2}\right) + \frac{k\delta f(x,y)}{n_0}V + \frac{kn_2I_0}{n_0}(|V|^2 + \alpha|U|^2)V = 0, \tag{1b}$$

where U and V are the normalized field envelopes, $k = 2\pi n_0/\lambda_0$, and the scaled function $f(x,y)$ represents the linear refractive index distribution of this waveguide network. In Eqs. (1), the term n_2I_0 stands for the maximum nonlinear index change induced by the beam right at the origin and, for simplicity, the self/cross-phase-modulation ratio α is taken here to be unity. Equations (1) are solved numerically using a beam propagation method, which allows one to exactly monitor any radiation and reflection losses in the network.

By using numerical relaxation methods, we then obtain discrete soliton solutions in this array system. As

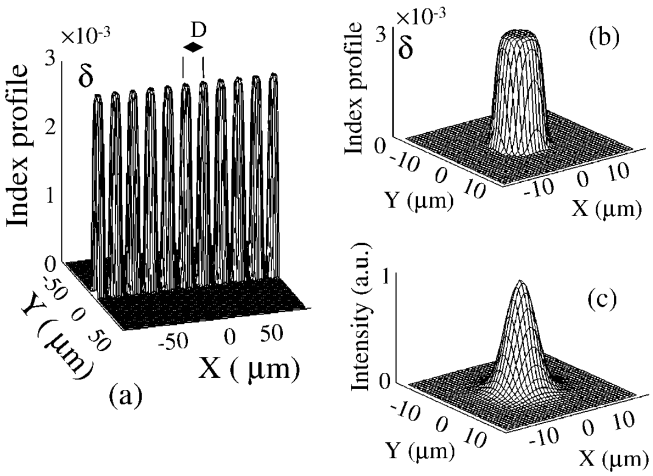

FIG. 1. (a) Refractive index distribution along a single row of waveguides; (b) refractive index profile of a single waveguide; (c) the fundamental waveguide mode intensity.

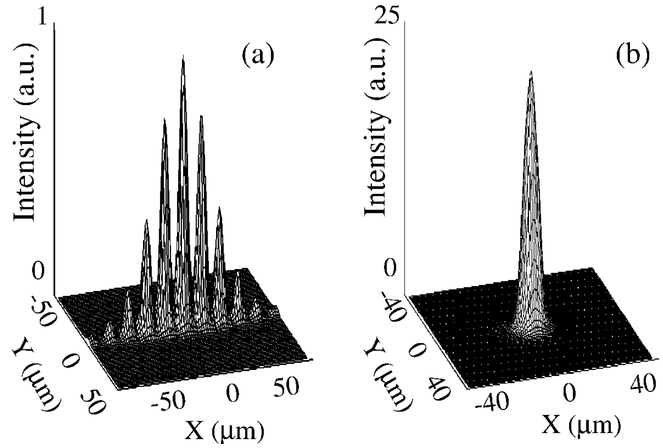

FIG. 2. (a) A moderately confined (signal) DS; (b) a strongly confined DS (blocker).

an initial trial function we use the discrete soliton solutions as obtained from coupled mode theory [2,15]. Here we isolate two classes of solitons: (i) moderately confined discrete solitons (hereby referred to as *signals*) and (ii) strongly confined soliton states, which we call *blockers*. A moderately confined soliton (essentially extending over 5–7 sites) residing on discrete waveguide sites is shown in Fig. 2(a). The maximum nonlinear index change required to support this soliton is $\Delta n_{\mathrm{NL}} = 4.6 \times 10^{-5} = n_2 I_0$. In this case, because of the relatively weak confinement, the maximum field amplitude at each lattice site approximately follows a hyperbolic secant envelope function $\Psi(n) = \Psi_0 \operatorname{sech}(nD/x_0)$, where $n = 0, \pm 1, \ldots$ is associated with the waveguide number, x_0 is the soliton width, and $\Psi(n)$ is the envelope function describing the peak intensities of U and V at the discrete sites [2]. In this regime, the soliton is highly mobile and its envelope is known to approximately obey a nonlinear Schrödinger equation. In the other extreme (for blockers), the field resides almost entirely in one waveguide and its envelope is described approximately by a defectlike state $\Psi(n) = \Psi_0 \exp(-|n|D/x_0)$. This latter class of solitons is known to exhibit much lower mobilities. The blocking soliton of Fig. 2(b) induces a maximum nonlinear index change of $\Delta n_{\mathrm{NL}} = 1 \times 10^{-3}$.

We then set a signal discrete soliton (Fig. 2a) in motion along the horizontal axis of a network which involves two array branches intersecting at 120°, as shown in Fig. 3(a). This is done by initially imposing a linear phase chirp (tilt) on the beam profile [5], i.e., $\Psi(n) = \Psi_0 \operatorname{sech}(nD/x_0)\exp(i\gamma n)$, where in our example the phase shift between neighboring sites is $\gamma = 0.6$ rad. Experimentally, this phase tilt can be provided by injecting the optical beam at an angle with respect to the array [10]. In all our simulations the value of γ was kept below $\pi/2$ so as to ensure distortionless propagation in the array, by avoiding higher order diffraction effects [10]. Under these conditions ($\gamma = 0.6$ rad), the soliton shifts its position by one waveguide site ($D = 15.9\ \mu$m) for every $z = 4.2$ mm of propagation. As a result the soliton slides along the horizontal branch and after passing the intersection moves to the upper branch. Figure 3(b) (obtained after 6.5 cm) shows that this occurred with almost no change in the soliton intensity profile or speed. Even more importantly, the losses because of the bend are extremely low (less than 0.7%). In other words, the soliton travels only along the network pathways, i.e., the array behaves like a *soliton wire*. These low levels of losses at 120° junctions suggest that discrete solitons can be effectively used as information carriers in homeycomblike networks. During propagation, the soliton exhibits robustness and it does not suffer from transverse modulational instability. This is because the soliton itself is linearly guided by the array in the direction normal to its motion. Similar results were obtained for a 90° bend, as depicted in Figs. 3(c) and 3(d). In this case, the soliton traverses the bend with a loss of 5%. Figure 3(d) depicts the soliton intensity after 6.4 cm of propagation (after the 90° bend), indicating that

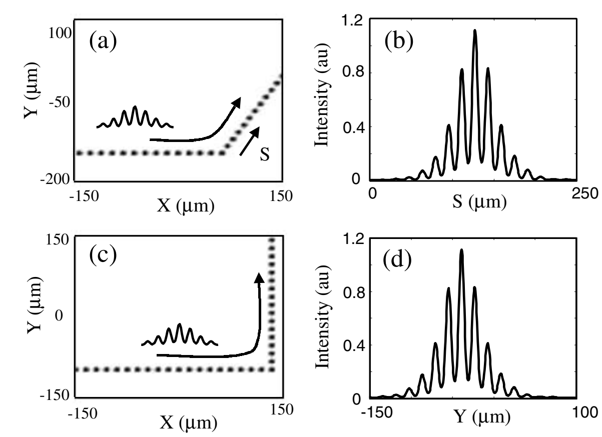

FIG. 3. (a) A signal DS, propagating along a 120° branch; (b) DS intensity at $z = 6.5$ cm (after traversing the bend); (c) same as (a) for a 90° bend; (d) DS intensity at 6.4 cm when the signal is already on the vertical branch.

the DS remained practically invariant. This behavior is to some extent reminiscent of that of waves propagating along sharp bends in photonic crystal waveguides [16]. Yet, unlike what happens in photonic crystals which use a high refractive index contrast, the process reported here requires a very small index difference δ. This is due to the fact that the DS soliton motion relies on optical tunneling, i.e., it slides at grazing angles. We then compared our results with those obtained using one-dimensional continuous solitons propagating obliquely in a planar waveguide system [17]. In this latter configuration, the soliton suffers a 30% loss and very quickly deteriorates after a 90° waveguide bend. This clearly indicates that DSs have a definite advantage over their continuous counterparts in such network arrangements.

Next we investigate how discrete solitons can be routed or blocked at network junctions using vector interactions. Figure 4(a) shows a Y-120° intersection involving three array branches. A DS of the blocking type [same as that of Fig. 2(b)] is positioned at site A, right at the entrance of the lower branch. A signal soliton, like that of Fig. 2(a), is then set in motion (from left to right) with $\gamma = 0.6$ rad, starting from position B. The two solitons are mutually incoherent, i.e., one is described by the U field and the other one by V in Eqs. (1). Our simulations indicate that the signal DS is routed to the upper branch in an elastic fashion. Figure 4(b) depicts the intensity of the signal DS at 5.68 cm (after passing the intersection). During this interaction, the blocker always remains in its preassigned position. The refractive index around the interaction region of these two DSs is mostly dominated by the high-intensity blocker. The junction losses, because of reflections and some small transmission to the lower branch, are in this case about 2%. In other words, the strongly confined DS blocks the lower pathway and *all optically routes* the signal soliton to the upper branch. Note that, had the blocker not been present at the junction, the signal DS would have totally disintegrated into transmitted and reflected waves ($\sim$30% per branch). Thus the presence of the blocking DS is extremely essential for this routing operation to occur. Similar results were obtained for T junctions, as shown in Fig. 4(c), using the same two families of mutually incoherent discrete solitons. When the blocker is present at position A, the signal is routed to the upper branch with an efficiency of 94.3%. Another basic element in such networks is an X junction, as shown in Fig. 4(d). Rerouting at this junction can be accomplished by using two blockers at positions A and B, thus cutting out two of the three output pathways. These two highly confined DSs are coherent with each other and are in antiphase ($\pm$) for stability purposes [18]. The signal in this case is routed to branch Q with an efficiency of 96%. The solitons used are again those of Fig. 2. This process requires both blockers to be present, otherwise the signal DS will disintegrate at the junction. Thus, essentially, the X junction functions as an AND logic gate, i.e., $Q = A \cdot B$. Again, during this interaction the two blockers remained in their preassigned positions. Finally, in addition to AND logic functions, a NOT logic gate ($Q = \bar{A}$) can be easily implemented by placing a blocker in the path of a signal DS provided that the two beams are mutually incoherent. We would like to stress that, in all examples discussed in this section, the blocker(s) must be interacting incoherently or vectorially with the signals. On the other hand, if these two classes of DSs are coherent with respect to each other [19], the blocking and routing actions at a junction are impaired, i.e., the interactions are no longer elastic. It is also perhaps worth noting that one can draw a strong parallelism between the all-optical blocking actions reported here and those occurring in abundance in biological systems [20]. For example, drugs are known to block synaptic neuron transmission by changing the synthesis of a specific neurotransmitter.

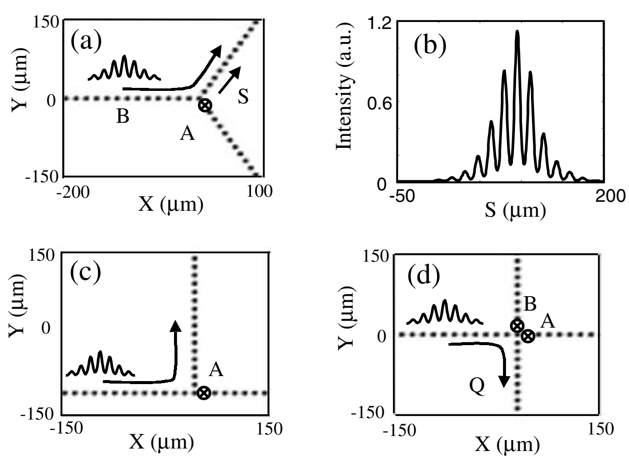

FIG. 4. (a) A signal DS routed by a blocker at position A; (b) intensity of the signal beam after 5.68 cm of propagation at $s = 95$ μm; (c) same as in (a) with a T junction; (d) an X junction blocked at sites A and B.

Time gating functions are also possible in such networks. Figure 5 shows a T junction with a blocker B placed at the intersection. A signal DS S, which is incoherent with respect to the blocker, travels from right to left towards the junction. At the same time, another signal soliton G, which is coherent with the blocker, moves toward the junction on the vertical branch. In our system the G wave reaches the junction before the S. Because

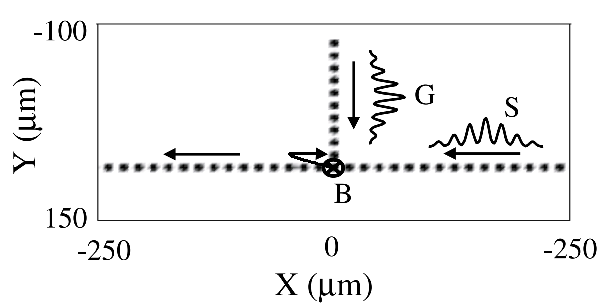

FIG. 5. A signal DS G pulling the blocker B just in time to allow the S soliton to pass through, thus performing time gating.

of the coherent interaction between the blocker and G, the blocker then moves discretely [19] by one slot upwards, just in time to allow the signal soliton to pass through.

We would like to emphasize that the results presented in our paper are possible over a wide range of parameters. For example, the transmission efficiency of the T junction shown in Fig. 4(c) remains above 90% for $0.25 < \gamma < 1$. Similarly, the transmission efficiency of the Y junction of Fig. 4(a) exceeds 90% provided that the blocker's Δn_{NL} is above 0.5×10^{-3} when $\gamma = 0.6$. In addition our results are insensitive to the particular choice of the waveguide profile, as long as each waveguide is designed to be single moded.

In conclusion, we have demonstrated that discrete optical solitons propagating in two-dimensional networks of waveguide arrays can provide a rich environment for all-optical data processing applications. These solitons can be navigated on predefined tracks (negotiating even sharp bends) and can be all optically routed anywhere in the network using vector interactions. Logic functions such as AND, NOT, and time gating are possible. The subsystems or building blocks involved are modular, i.e., they can be replicated anywhere in the network. In addition, these two-dimensional waveguide array systems are compatible with photonic crystal technologies [16,21]. Even more importantly, such a system has the flexibility of exploiting both coherent and incoherent interactions and, in principle, N mutually incoherent field components can be involved [13]. Coherent collisions lead to disrete spatial shifts, whereas incoherent interactions allow for elastic collisions and leave the blocking DSs in their preassigned positions. The possibility of implementing all-optical routers and memory functions using such networks is currently under investigation.

Animations of the processes described in Figs. 3–5, as obtained by numerically solving Eqs. (1), can also be viewed; see Ref. [22].

This work was supported by an ARO MURI, the National Science Foundation, and by a grant from the Pittsburgh Supercomputing Center.

[1] A. C. Scott, Philos. Trans. R. Soc. London A **315**, 423 (1985); A. S. Davydov, *Biology and Quantum Mechanics* (Pergamon, Oxford, 1982).

[2] D. N. Christodoulides and R. I. Joseph, Opt. Lett. **13**, 794 (1988).

[3] D. Cai, A. R. Bishop, and N. Grønbech-Jensen, Phys. Rev. Lett. **72**, 591 (1994).

[4] A. Trombettoni and A. Smerzi, Phys. Rev. Lett. **86**, 2353 (2001).

[5] H. S. Eisenberg, Y. Silberberg, R. Morandotti, A. R. Boyd, and J. S. Aitchison, Phys. Rev. Lett. **81**, 3383 (1998); R. Morandotti, U. Peschel, J. S. Aitchison, H. S. Eisenberg, and Y. Silberberg, Phys. Rev. Lett. **83**, 2726 (1999).

[6] R. Muschall, C. Schmidt-Hattenberger, and F. Lederer, Opt. Lett. **19**, 323 (1994).

[7] Y. S. Kivshar and D. K. Campbell, Phys. Rev. E **48**, 3077 (1993); W. Krolikowski and Y. S. Kivshar, J. Opt. Soc. Am. B **13**, 876 (1996); Y. S. Kivshar, Opt. Lett. **18**, 1147 (1993).

[8] A. B. Aceves and C. De Angelis, T. Peschel, R. Muschall, F. Lederer, S. Trillo, and S. Wabnitz, Phys. Rev. E **53**, 1172 (1996).

[9] S. Darmanyan, A. Kobyakov, E. Schmidt, and F. Lederer, Phys. Rev. E **57**, 3520 (1998).

[10] H. S. Eisenberg, Y. Silberberg, R. Morandotti, and J. S. Aitchison, Phys. Rev. Lett. **85**, 1863 (2000); R. Morandotti, H. S. Eisenberg, Y. Silberberg, M. Sorel, and J. S. Aitchison, Phys. Rev. Lett. **86**, 3296 (2001).

[11] A. W. Snyder and J. D. Love, *Optical Waveguide Theory* (Chapman and Hall, New York, 1983). In our work the normalized index profile of each waveguide was taken to be $e^{-(r/a)^8}$ with $a = 5.3$ μm so as to be single moded.

[12] In materials with electronic nonlinearities, vector/incoherent interactions can be accomplished by either using two different polarizations in anisotropic systems ($\alpha = 2/3$) or using two different colors, in which case $\alpha = 2$. See, for example, G. P. Agrawal, *Nonlinear Fiber Optics* (Academic, San Diego, 1995).

[13] Incoherent interactions with an arbitrary number of components can also be realized in photorefractives, e.g., D. N. Christodoulides, S. R. Singh, M. I. Carvalho, and M. Segev, Appl. Phys. Lett. **68**, 1763 (1996), and in $\chi^{(2)}$ media, e.g., V. V. Steblina, A. V. Buryak, R. A. Sammut, D. Zhou, M. Segev, and P. Prucnal, J. Opt. Soc. B **17**, 2026 (2000).

[14] G. I. Stegeman and M. Segev, Science **286**, 1518 (1999); M. Segev and G. I. Stegeman, Phys. Today **51**, No. 8, 42 (1998).

[15] A. C. Scott and L. Macneil, Phys. Lett. A **98**, 87 (1983).

[16] J. D. Joannopoulos, P. R. Villeneuve, and S. Fan, Nature (London) **386**, 143 (1997).

[17] J. S. Aitchison *et al.,* Opt. Lett. **15**, 471 (1990).

[18] B. Daino, G. Gregory, and S. Wabnitz, J. Appl. Phys. **58**, 4512 (1985); H. G. Winful, Opt. Lett. **11**, 33 (1986). Note that the two-blocker arrangement in Fig. 4(d) is stable even for phase shifts between $2\pi/3$ and $4\pi/3$.

[19] O. Bang and P. D. Miller, Opt. Lett. **21**, 1105 (1996).

[20] T. Blackmer, E. C. Larsen, M. Takhashi, T. F. J. Martin, S. Alford, and H. E. Hamm, Science **292**, 293 (2001); W. G. Richards, *Quantum Pharmacology* (Butterworths, London, 1977).

[21] S. F. Mingaleev, Y. S. Kivshar, and R. A. Sammut, Phys. Rev. E **62**, 5777 (2000).

[22] See AIP Document No. EPAPS: E-PRLTAO-87-018147 for animations of processes described in Figs. 3–5, as obtained numerically by solving Eqs. (1). This document may be retrieved via the EPAPS homepage (http://www.aip.org/pubservs/epaps.html) or from ftp.aip.org in the directory /epaps/. See the EPAPS homepage for more information.